energies

MDPI

Article

A Method for Increasing the Operating Limit Capacity of Wind Farms Using Battery Energy Storage Systems with Rate of Change of Frequency

Dae-Hee Son [1], Muhammad Ali [1], Sang-Hee Kang [1], Jae-Haeng Heo [2] and Soon-Ryul Nam [1,*]

[1] Department of Electrical Engineering, 3rd Engineering Structure, Myongji University, 116 Myongji-ro, Cheoin-gu, Yongin-si, Gyeonggi-do 17058, Korea; sonking18@nate.com (D.-H.S.); friendsspecial.ali@gmail.com (M.A.); shkang@mju.ac.kr (S.-H.K.)

[2] Raon Friends, 267 Simi-daero, Dongan-gu, Anyang-si, Gyeonggi-do 14054, Korea; jhheo78@gmail.com

* Correspondence: ptsouth@mju.ac.kr; Tel.: +82-31-330-6361

Received: 28 February 2018; Accepted: 23 March 2018; Published: 27 March 2018

Abstract: In this paper, the appropriate rated power of battery energy storage system (BESS) and the operating limit capacity of wind farms are determined considering power system stability, and novel output control methods of BESS and wind turbines are proposed. The rated power of BESS is determined by correlation with the kinetic energy that can be released from wind turbines and synchronous generators when a disturbance occurs in the power system. After the appropriate rated power of BESS is determined, a novel control scheme for quickly responding to disturbances should be applied to BESS. It is important to compensate the insufficient power difference between demand and supply more quickly after a disturbance, and for this purpose, BESS output is controlled using the rate of change of frequency (ROCOF). Generally, BESS output is controlled by the frequency droop control (FDC), however if ROCOF falls below the threshold, BESS output increases sharply. Under this control for BESS, the power system's stability can be improved and the operating limit capacity of wind farms can be increased. The operating limit capacity is determined as the smaller of technical limit and dynamic limit capacity. The technical limit capacity is calculated by the difference between the maximum power of the generators connected to the power system and the magnitude of loads, and the dynamic limit capacity is determined by considering dynamic stability of a power system frequency when the wind turbines drop out from a power system. Output of the dynamic model developed for wind turbine is based on the operating limit capacity and is controlled by blade pitch angle. To validate the effectiveness of the proposed control method, different case studies are conducted, with simulations for BESS and wind turbine using Power System Simulation for Engineering (PSS/E).

Keywords: battery energy storage system (BESS); kinetic energy; rate of change of frequency (ROCOF); operating limit capacity; blade pitch angle

1. Introduction

In recent year, renewable generators such as solar photovoltaic (PV), and wind turbines have received significant attention in power systems. Among the types of renewable generators, wind turbines are some of the most attractive renewable generators in many countries due to their technical and economic feasibility. Global wind power generation increased by 54,600 MW in 2016, and the total by the end of the year was 486.8 GW, representing a cumulative market growth of more than 12 percent. South Korea had a total wind turbine capacity of just over 1000 MW following the installation of 200 MW new generators in 2016 [1]; however, this wind turbine capacity is still insufficient compared

with that in other energy advanced countries. Hence, Korea Power Exchange (KPX: the wholesale electricity market operator for South Korea) has a long term plan to increase the proportion of new and renewable power generation in accordance with the 8th basic plan of South Korea. The cumulative capacity of renewable generators in the 8th basic plan is 58,461 MW by the year 2030, of which the wind turbine capacity is 17,674 MW [2]. To install wind turbines for power generation, it is essential to select a feasible site, typically, windy islands or mountainous areas. Jeju island has the highest average wind speed in South Korea, with an annual wind speed on the east and west coasts of about 7 m/s [3,4]. Good wind conditions have led to increasing wind power generation, and public and the Jeju Energy Corporation (JEC: Jeju island Energy Institute of Technology Corporation in Jeju Special Self-Governing Province, Jeju-city, Jeju-do, Korea) of Jeju Province projects that by 2030, offshore wind power generation will rise to 2 GW [5].

Increasing wind power generation has some advantages such as reduced pollutant emissions and economic benefits; however, large-scale penetration of wind turbines can adversely affect the stability of power systems. The irregular wind speed causes fluctuations in wind power generation, which may lead to unbalanced power supply and demand [6–8]. The power system stability therefore need to be considered when installing wind turbines. Several previous studies have investigated the increasing penetration of wind turbines based on a transient operation of the power system. Above all, a method has been developed to calculate the operating limit capacity of wind farms according to the system situation. The operating limit capacity is determined by the minimum value of the technical limit capacity from the difference between minimum and maximum power of penetrated generators and the dynamic limit capacity by the simulation for stability [9,10].

To mitigate the power fluctuations in wind power generation, an Energy Storage System (ESS) is used in the power system. In particular, batteries are widely used for ESS, which constitute a Battery Energy Storage System (BESS). Although South Korea is one of the world's leading battery manufacturers, the country has little experience in BESS technologies such as flywheel and flow batteries [11]. Nevertheless, to increase the penetration of wind turbines, appropriate BESS technologies should be developed. BESS can help the primary frequency response against frequency deviations due to the fast response characteristics of batteries when the disturbance such as large-scale wind farm loss occurs [12–16]. Previously, the BESS output has been controlled by the Frequency Droop Control (FDC) to respond to frequency deviations [17,18]; however, the FDC does not effectively use the fast output characteristics of BESS. Hence, Rate of Change of Frequency (ROCOF) is used for control BESS output to respond to any power disturbance more quickly [14,19,20]. When ROCOF falls below the threshold, BESS outputs the maximum value of that. In this case, it is necessary to calculate the appropriate rated power of BESS according to the state of the power system to prevent power over-compensation or under-compensation. Therefore, this paper proposes a calculation method of the appropriate rated power of BESS and a flexible output control using ROCOF. At the beginning of a transient caused by a disturbance such as a load increase and loss of generators, the rated power of BESS was estimated by releasable kinetic energy from the remaining generators [16]. Initial ROCOF is determined by the magnitude of the initial power difference between supply and demand [14,21,22]; then, the larger the power deviation, the more the ROCOF falls. Using this function, it is possible to estimate the threshold of ROCOF for a specific power deviation that affects the power system stability. If ROCOF falls below the threshold value, BESS quickly outputs the appropriate power. Therefore, the power system stability can be improved by BESS using ROCOF.

In this paper, the operating limit capacity of the wind farms is increased by attaching BESS to the power system and controlling this using ROCOF. When the wind power generation fluctuates due to a change in wind speed, BESS controlled by using ROCOF is used to compensate the insufficient power quickly, and the frequency transient state is mitigated. In this way, the operating limit capacity of the wind farms can be increased. Once the capacity of a wind farms is determined, the output power of wind turbines is controlled by the pitch angle control depending on the operating limit capacity [23–26]. In this paper, the above theory is summarized and proved by using the Jeju island

power system. As shown Figure 1, the Seongsan wind farm is connected to the Seongsan S/S east side of the Jeju island and the Hanrim wind farm is connected to the Hanrim S/S west side of Jeju island. BESS also is connected to the Hanrim S/S because the Hanrim wind farm is excluded from the power system on the simulation. To perform the simulation, Power System Simulation for Engineering (PSS/E: the software for power system analysis) was used, and BESS and wind turbine model are user-defined model coded in FORTRAN, respectively [27–30].

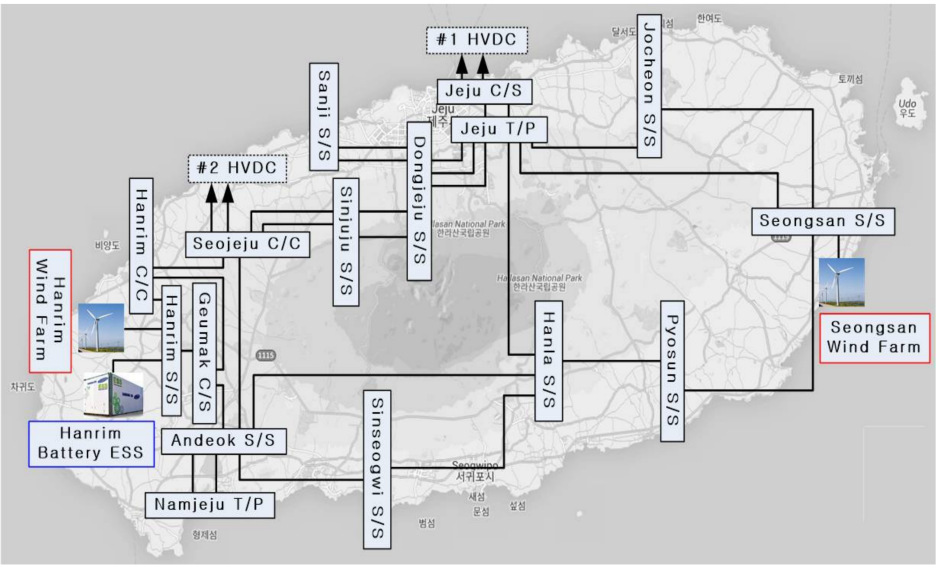

Figure 1. Jeju island power system with wind farms and battery [31].

2. Operation Method of BESS for Frequency Response

To connect BESS with wind farm, it is essential to determine the appropriate rated power and control schemes of BESS. Hence, in this section, we will define a method for calculating the rated power and output control scheme of BESS.

2.1. Calculations for the Rated Power of BESS

To operate power system effectively and economically with BESS, it is important to determine the appropriate rated power of BESS for the power system. If the rated power of BESS is more than the requirement, economic losses due to excessive battery installation costs and power instability due to extreme power compensation occur. In the opposite case, BESS can't fulfill its frequency regulation role. In this paper, the appropriate rated power of BESS is calculated by citing reference [16] on power system characteristics.

When a synchronous generator is operated under the rated state, the kinetic energy E_k^{SG} stored in the rotor is:

$$E_k = \frac{1}{2} J \omega_s^2 = \frac{1}{2} P_N T_J (T_J = 2H) \tag{1}$$

where J is the moment of inertia of the generators, ω_s is the synchronous speed, P_N is the rated power of generator and T_J is the inertia time constant, which is equal to $2H$. The kinetic energy of synchronous generator varies with the change in the system frequency. In this paper, the permissible instantaneous maximum frequency deviation of the power system is determined as 60 ± 0.3 Hz $(1.0 \pm 0.005$ pu$)$ with reference to [32]; then, the permissible maximum deviation of kinetic energy $\Delta E_{k\,\max}^{SG}$ is expressed by Equation (2):

$$\Delta E_{k\,\max}^{SG} = \frac{1}{2} J (1 - 0.995^2) \omega_s^2 = \frac{1}{2} \times 0.009975 J \omega_s^2 = \frac{1}{2} \times 0.009975 P_N^{SG} T_J^{SG} \tag{2}$$

This kinetic energy deviation is allowed in the power system when any disturbance occurs in a transient state. When the wind turbines are excluded from the power system, the total kinetic energy without the permissible energy deviation of the lost wind turbines ΔE^{W}_{Total} is:

$$\Delta E^{W}_{Total} = \frac{1}{2}J(0.995^2 - 1)\omega_s^2 = \frac{1}{2} \times 0.0990025 J\omega_s^2 = \frac{1}{2} \times 0.990025 P^{W}_{N} T^{W}_{J} \tag{3}$$

BESS and other synchronous generators should compensate the insufficient power between supply and demand after losing wind turbines. Therefore, the released energy from BESS during the period $0 \sim t_1$ is the same as difference between the total kinetic energy of the lost wind turbines and the permissible energy deviation of the other synchronous generator:

$$\Delta E_{BESS} = \Delta E^{W}_{Total} - \Delta E^{SG}_{k\max} = \int_0^{t_1} P_{BESS}(t)\, dt \; = P_{MBESS} t_1 \tag{4}$$

In the Equation (4), ΔE_{BESS} is the released energy of BESS, P_{BESS} is the power of BESS and P_{MBESS} is the mean power value of BESS. By rearranging (4), the mean power value of BESS is:

$$P_{MBESS} = \frac{\Delta E^{W}_{k} - \Delta E^{SG}_{Total}}{t_1} = \frac{0.5 \times 0.990025 P^{W}_{N} T^{W}_{J}}{t_1} - \frac{0.5 \times 0.009975 P^{SG}_{N} T^{SG}_{J}}{t_1} \tag{5}$$

The power of BESS $P^{\max}_{BESS}(t)$ is not less than mean power value P_{MBESS}, and the rated power of BESS P_{NBESS} should also not be less than $P^{\max}_{BESS}(t)$. Therefore, the mean power value P_{MBESS} is the theoretical minimum value of the rated power of BESS, the rated power of BESS is determined by:

$$P_{NBESS} \approx 0.495 P^{W}_{N} \frac{T^{W}_{J}}{t_1} - 0.005 P^{SG}_{N} \frac{T^{SG}_{J}}{t_1} \tag{6}$$

Typically, a larger inertia time constant T_J will lead to a larger t_1. The inertia time constant T_J of synchronous generators is in the range of 4–18 s [16], and the time t_1 is for the system to reach the maximum frequency deviation after disturbance, usually 7–15 s [33]. Therefore, the time t_1 is approximately equal to the inertia time constant T_J. Consequently, the rated power of BESS is determined in the way given by Equation (7):

$$P_{NBESS} \approx 0.495 P^{W}_{N} - 0.005 P^{SG}_{N} \tag{7}$$

where the rated power of BESS is determined as the difference between 49.5% of wind farm and 0.5% of the synchronous generators.

2.2. BESS Output Control for Frequency Response

2.2.1. BESS Output Using FDC

Frequency Droop Control (FDC) is the basic control method for controlling BESS. Therefore, we calculated BESS output with FDC and confirmed the effect to the power system stability. Figure 2 shows BESS output according to FDC. FDC is to increase BESS output in proportion to magnitude of frequency deviation from the rated system frequency. BESS with FDC is operated when the system frequency is out of the Dead Band (DB):

$$\begin{aligned} P_{BESS} &= k_1(f - f_n - f_{dead1}) \cdots (f - f_n < f_{dead1}) \\ P_{BESS} &= 0 \cdots\cdots\cdots\cdots\cdots (f_{dead1} < f - f_n < f_{dead2}) \\ P_{BESS} &= k_2(f - f_n - f_{dead2}) \cdots (f - f_n > f_{dead2}) \end{aligned} \tag{8}$$

P_{BESS} is the BESS output, k_1 and k_1 are the coefficients of frequency droop. In this paper, the coefficient of frequency droop is set to 0.5% because the BESS output power is at a maximum at

59.7 Hz. The system permissible instantaneous frequency in the transient state after disturbance is 59.7 Hz. f_n is the rated frequency of the system 60 Hz in South Korea, f is measured frequency. $f_{dead\ 1}$, $f_{dead\ 2}$ are the DB of FDC, range of DB is determined as 60 $\pm$ 0.017 Hz [34]. A user-defined model was developed in PSS/E based on (8) for FDC.

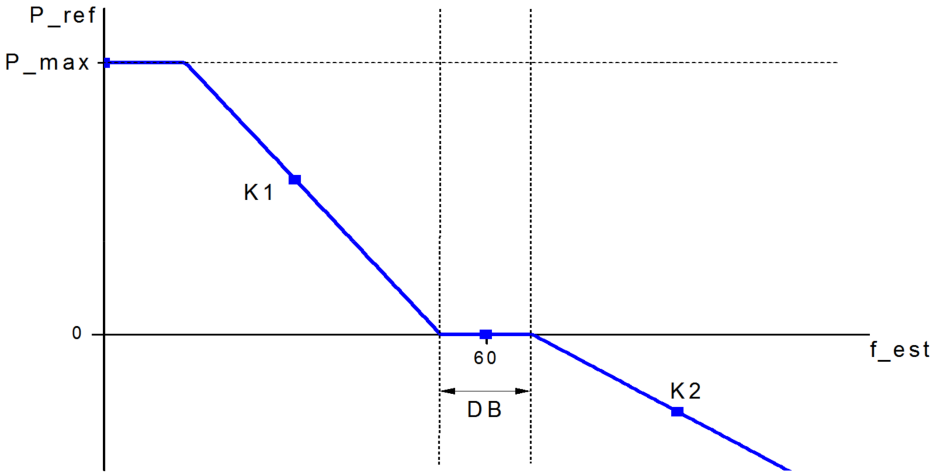

Figure 2. Battery energy storage system (BESS) output with Frequency Droop Control (FDC) according to the power system frequency [14].

2.2.2. BESS Output Using ROCOF

To improve the system stability, any power deviation between supply and demand should be compensated for more quickly after a rapid increase in load or loss in generating units; to this end, the method using ROCOF should be applied to BESS output control. A greater power deviation means a greater drop in ROCOF. Thus, BESS output is increased in proportion to the magnitude of the drop in ROCOF when ROCOF falls below the threshold. Normally, BESS output is controlled by FDC.

Figure 3 shows the operational sequence for BESS. First, BESS output is increased in proportion to the magnitude of ROCOF deviation from 0 Hz/s when ROCOF falls below the threshold (a). After that, BESS output remains constant while ROCOF is increased because this time is required to increase the output of the other generators (b). Once other generator's reserve power is inserted, BESS output should be slowly decreased to reduce the impact on the system stability (c).

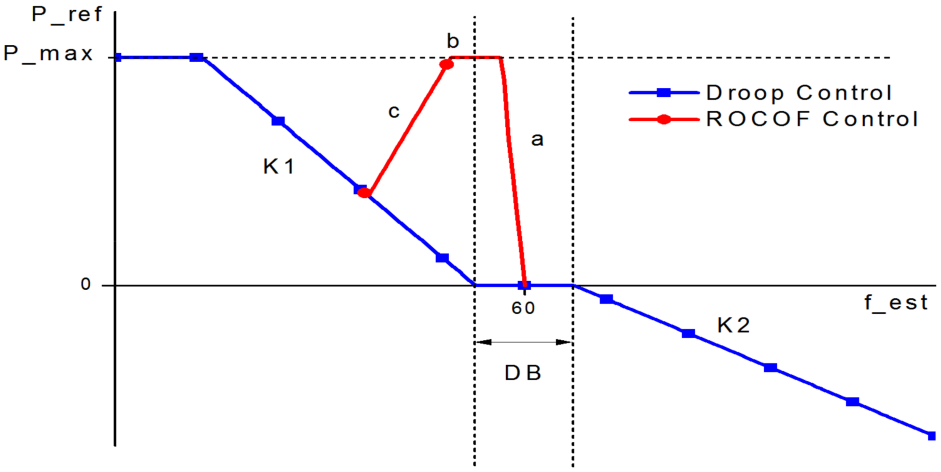

Figure 3. BESS output graph with FDC according to the system frequency and using Rate of Change of Frequency (ROCOF) [14].

Before applying ROCOF control to BESS, the thresholds value should be determined. When ROCOF is lower than the thresholds, BESS using ROCOF control is operated. The threshold of ROCOF is associated with the power deviation between supply and demand. The time derivative Δf can be estimated as [14]:

$$\frac{d\Delta f}{dt} = f_0 \frac{P_m(t) - P_e(t)}{2E_{Keq}} = f_0 \frac{\Delta\, P(t)}{2E_{Keq}} \tag{8}$$

where E_{Keq}[MWs] is the total kinetic energy stored at rated speed in the rotating masses of the generator, and $P_m(t)$ and $P_e(t)$ [MW] are the power generation and demand. Equation (8) is expressed in Equation (9) [14]:

$$\frac{d\Delta\, f}{dt} = f_0 \frac{\Delta P^{pu}(t)}{2H_{eq}} = f_0 \frac{\Delta\, P^{pu}(t)}{2M_{eq}} \tag{9}$$

$H_{eq} = E_{Keq}/VA_{base}$[MWs/MVA] and M_{eq}[s] are the equivalent inertia and mechanical start time constants of the considered power system. The total time constant of generators connected to the power system is given by the following Table 1 (The base is 100 MVA).

Table 1. Inertia time constants of each generator.

Generators	Inertia Time Constants [MWs/MVA]
Jeju GT#1	1.30
Jeju GT#2	1.30
Jeju TP#2	5.24
Jeju TP#3	5.24
Jeju DP#1	3.02
Jeju DP#2	3.02
Hanrim GT#1	3.00
Hanrim GT#2	3.00
Hanrim ST#1	3.00
South Jeju TP#3	7.71
South Jeju TP#4	7.71
Total	43.54

Initial power deviation of the ROCOF control for BESS operation is determined from the permissible maximum deviation of kinetic energy of synchronous generators in the power system. Equation (11) can be derived from Equation (2):

$$P_{Init} = \frac{\Delta E^{SG}_{kmax}}{t_1} = \frac{0.5 \times 0.009975 P^{SG}_N T^{SG}_J}{t_1} \cong 0.005 P^{SG}_N \tag{10}$$

Therefore, the initial power deviation is determined to be about 4 MW (0.04 pu) because the total rated power of generators in the Jeju island power system is 880 MW. The threshold of ROCOF control operation is determined as:

$$\frac{d\Delta\, f}{dt}(t) = f_0 \frac{\Delta P^{pu}(t)}{2H_{eq}} = 60 \times \frac{-0.04}{2 \times 43.54} = -0.028\ Hz/s \tag{11}$$

BESS output using ROCOF control increases in proportion to the magnitude of ROCOF drop and BESS output is set as 2 MW, which is half of the initial power when ROCOF is -0.028 Hz/s.

2.2.3. Case Study of BESS Output

To confirm the effect of FDC and ROCOF control, we have used CBEST BESS model supplied in Power System Simulation for Engineering (PSS/E) and simulated several cases. The structure of the CBEST BESS model is shown in Figure 4.

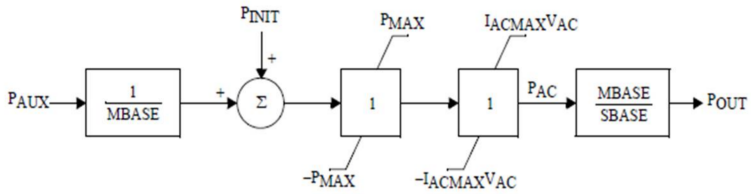

Figure 4. Diagram of CBEST BESS model from PSS/E [28].

The CBEST BESS output is controlled by P_{AUX} and P_{INIT}. P_{AUX} is the input value and P_{INIT} is the initial value of the CBEST BESS model. The others are values of output range. In this paper, initial value P_{INIT} is set as 0 because it is impossible to control the P_{INIT}. Therefore, only the input value P_{AUX} is set by FDC. The other setting values are shown in [35]. The initial load of the Jeju power system is set as 709 MW and the rated power of wind farm is set as 112.5 MW. Then, the rated power of CBEST BESS model is set as 51.5 MW, and the initial output is set as 0 MW. CBEST BESS model is connected to the Hanrim S/S in the Jeju power system.

As shown in Figure 5, after 30 s of simulation, the system load is increased by 2 MW to confirm the DB for FDC and ROCOF threshold. Consequently, there is no BESS output and the power system frequency changes in the same way as the no-BESS scenario because the nadir of the power system frequency is 59.995 Hz, within the DB and nadir ROCOF is −0.0124 Hz/s, above the threshold. In this case, BESS output using FDC and ROCOF is not operated.

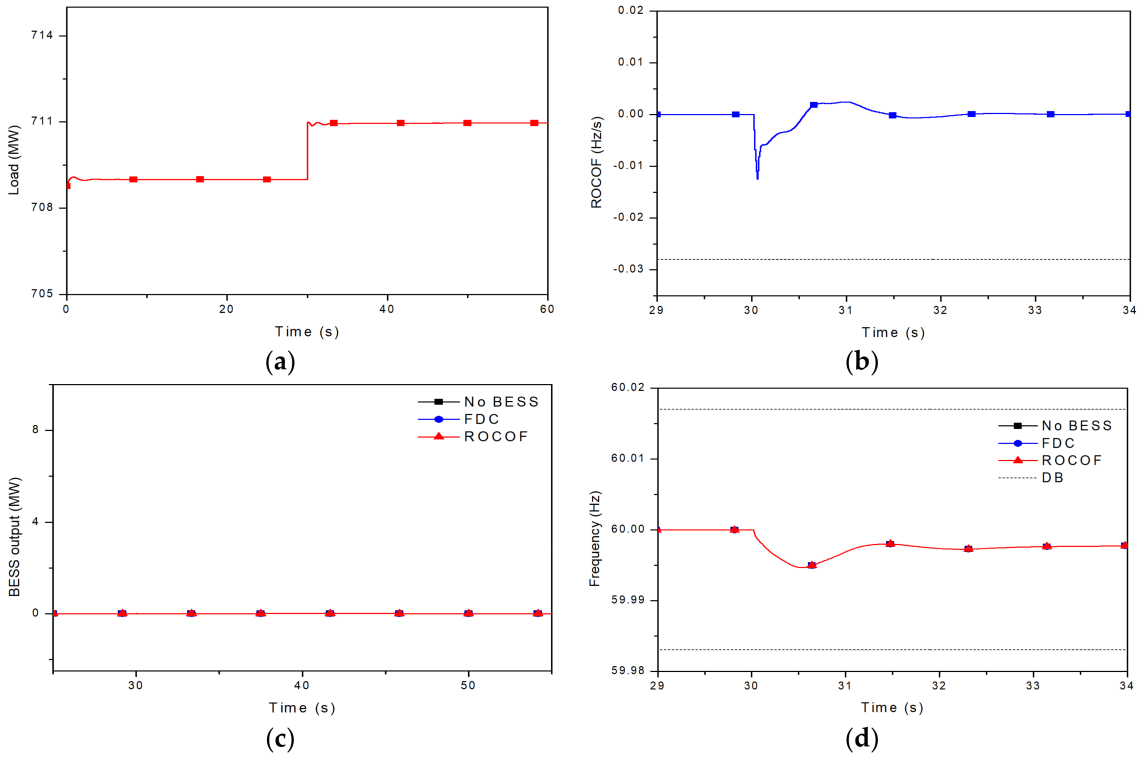

Figure 5. Power system load is increased by 2 MW: (**a**) Power system load; (**b**) Rate of Change of Frequency (ROCOF); (**c**) BESS output; (**d**) Power system frequency.

As shown in Figure 6, after 60 s, the system load is increased by 5% (=35.5 MW) of total load to compare BESS with FDC and ROCOF control operation when the system frequency is out of the DB and ROCOF is below the threshold. BESS with FDC output is increased in proportion to the deviation of the system frequency, so BESS with FDC improves the system frequency stability by compensating the power deviation between supply and demand more quickly than no BESS. BESS using ROCOF

output is increased in proportion to the magnitude of ROCOF deviation from 0 Hz/s. When ROCOF is below the threshold, BESS output is immediately increased because the power deviation should be more quickly compensated than BESS with FDC. Thus, Figure 6d confirms that the power system frequency stability should be more improved by using ROCOF. However, once ROCOF falls below the threshold, since BESS is operated according to the operation order, ROCOF does not affect BESS operation even though ROCOF again falls below the threshold during BESS operation in that order.

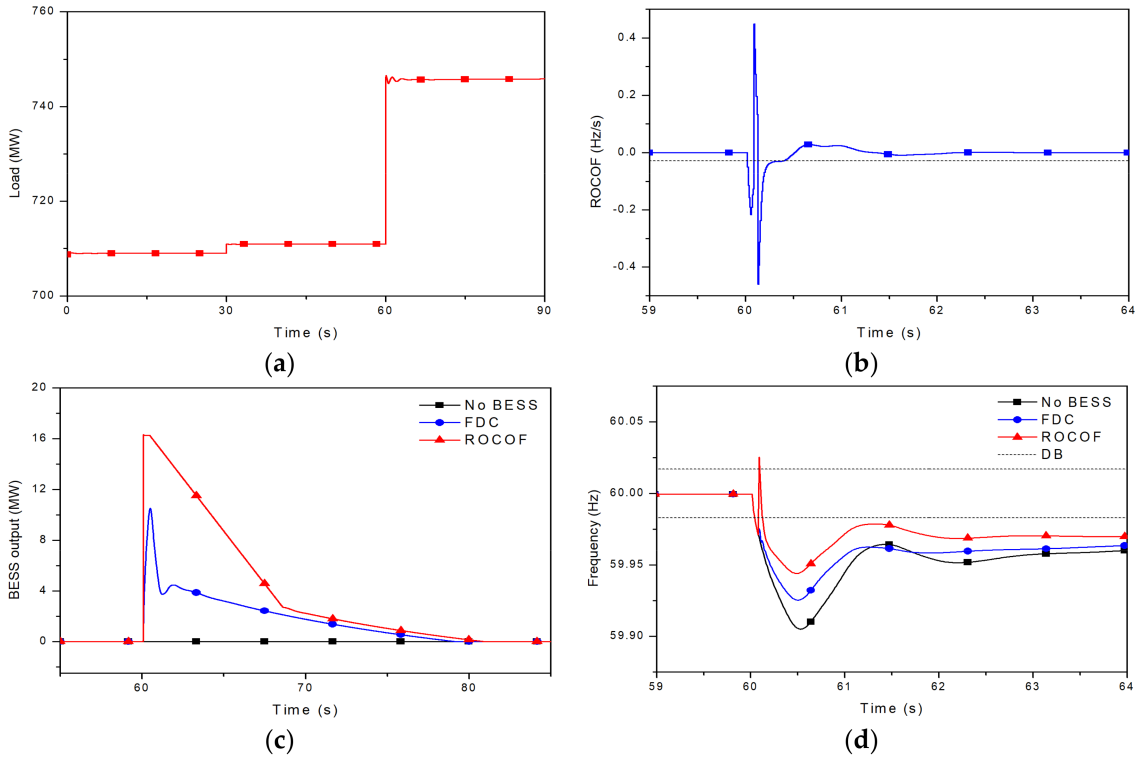

Figure 6. Power system load is increased by 5%: (**a**) Power system load; (**b**) Rate of Change of Frequency (ROCOF); (**c**) BESS output; (**d**) Power system frequency.

In conclusion, the system frequency stability can be improved by using ROCOF to compensate the power deviation more quickly in the transient state. In the next section, the operation limit capacity of wind farms will be determined in the Jeju island with BESS using ROCOF.

3. Wind Turbine Control Based on the Operating Limit Capacity

The output of wind turbine is unstable due to the variation of wind speed. Therefore, it is essential to determine the operating limit capacity of wind farms and control the wind turbine output considering the power system stability. In this section, the operating limit capacity of wind farms is calculated and the control method is proposed for wind turbine in Jeju island power system.

3.1. Calculations for Operating Limit of Wind Farm

The appropriate operating limit capacity should be calculated in the power system in consideration of economic efficiency and stability. The calculated operating limit capacity is the standard for wind turbine output. The operating limit capacity $P^O_{\max}$ of wind farms is determined as minimum value of the technical limit $P^T_{\max}$ and the dynamic limit capacity $P^D_{\max}$:

$$P^O_{\max} = \min(P^T_{\max},\ P^D_{\max}) \tag{12}$$

The technical limit and dynamic limit capacity are described in Sections 3.1.1 and 3.1.2, respectively.

3.1.1. The Technical Limit Capacity of Wind Farms

The technical limit capacity $P^T_{\max}$ is determined by the difference between the system load P_L and the sum of minimum power of generators which were connected to power system $\sum_k c_k P_k$:

$$P^T_{\max} = P_L - \sum_k c_k P_k \tag{13}$$

To prevent wear and improve the efficiency of power generation, each generator should output the power generation over a certain value. Accordingly, the minimum power generation rate c_k is usually 30~50% of the rated power depending on the generator type [9]. The technical limit capacity $P^T_{\max}$ with the minimum power generation rate c_k is:

$$P^T_{\max} = P_L - \sum_k c_k P_k = \sum_k P_k - \sum_k c_k P_k \tag{14}$$

The generation units with merit order 1 are penetrated into the Jeju power system. The generation units in Table 2 are penetrated step by step when the system load P_L is over the rated power of penetrated generators. The technical limit capacity $P^T_{\max}$ is determined by the difference between the system load P_L and the minimum power of penetrated generators on each step. Thus, the technical limit capacity $P^T_{\max}$ is given:

$$P^T_{\max}(1) = P_L - 284 \text{ MW } (284 \text{ MW} \le P_L < 550 \text{ MW}) \tag{15}$$

$$P^T_{\max}(2) = P_L - 334 \text{ MW } (550 \text{ MW} \le P_L < 650 \text{ MW}) \tag{16}$$

$$P^T_{\max}(3) = P_L - 484 \text{ MW } (650 \text{ MW} \le P_L < 800 \text{ MW}) \tag{17}$$

$$P^T_{\max}(4) = P_L - 510 \text{ MW } (800 \text{ MW} \le P_L < 840 \text{ MW}) \tag{18}$$

$$P^T_{\max}(5) = P_L - 536 \text{ MW } (840 \text{ MW} \le P_L < 880 \text{ MW}) \tag{19}$$

Table 2. Rate power and minimum power of generation units.

Merit Order	Generation Unit	Rate Power	Minimum Power
1	HVDC#1	150	75
1	HVDC#2	150	75
1	Jeju TP#2	75	42
1	Jeju TP#3	75	42
1	South Jeju TP#4	100	50
2	South Jeju TP#3	100	50
3	HVDC#5	75	75
3	HVDC#6	75	75
4	Jeju DP#1	40	26
5	Jeju DP#2	40	26

According to the above equation, the technical limit capacity $P^T_{\max}$ is shown in Figure 7.

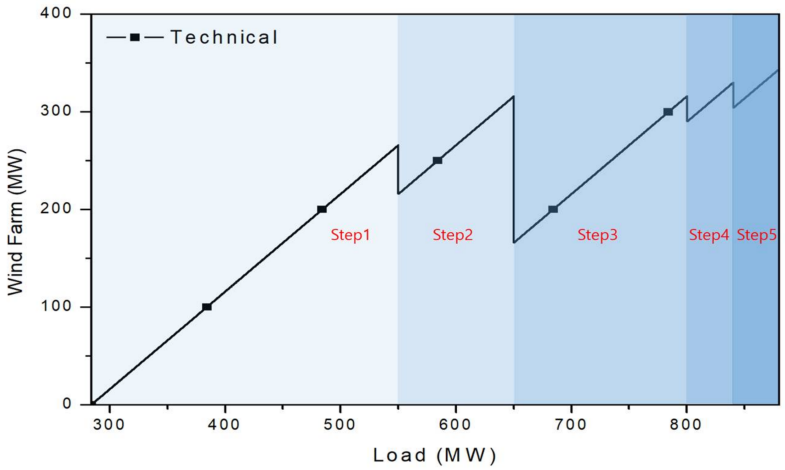

Figure 7. The technical limit capacity of wind farms in Jeju island.

3.1.2. The Dynamic Limit Capacity of Wind Farms

Wind turbines have characteristic that large-scale wind turbines are able to fall out of the power system at the same time. If a power system is vulnerable, the capacity of wind farms should be restricted such that it does exceed a certain rate in consideration of the power system stability. The dynamic limit capacity $P^D_{\max}$ of wind farms is determined by simulations on wind turbines loss from the power system. The wind generators are increased step by step within the range where the system frequency does not fall below 59.7 Hz because the instantaneous minimum frequency reference is 59.7 Hz [32] in the power system. In the Jeju power system, the wind farm model is connected to Seongsan S/S in the east and Hanrim S/S in the west and BESS is also connected to Hanrim S/S for the simulation. It is simulated that only the wind turbines of Hanrim S/S is lost, then, HVDC, other conventional generators and BESS compensate insufficient power. The dynamic limit capacity of the power system depends on BESS output control method or the situation without BESS. To compare the respective result, the same power of wind farm (48 MW) was dropped out from the power system. The wind farms of both regions were not lost simultaneously at the same time, the capacity of both wind farms is same.

When the wind turbines are lost, BESS using ROCOF more quickly compensates for insufficient power to the power system than BESS with FDC as shown in Figure 8. Therefore, since BESS using ROCOF can contribute an increase in the dynamic limit capacity, it is applied to determine the dynamic limit capacity $P^D_{\max}$. Each step's the dynamic limit capacity $P^D_{\max}$ is determined at each generator penetration step.

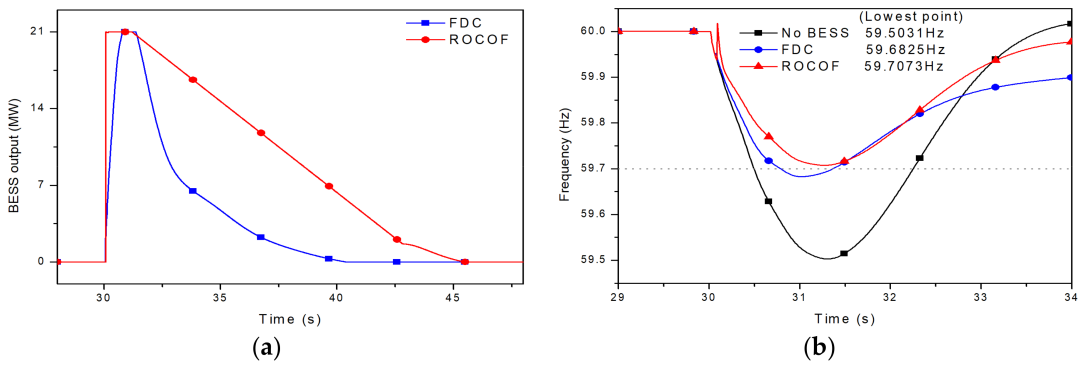

Figure 8. Power system frequency according to BESS output control when wind turbine is lost: (**a**) BESS output; (**b**) Frequency of the power system.

A wind farm with 48 MW was connected to each of Hanrim S/S and Seongsan S/S, and the wind farm at Hanrim S/S is lost after 30 s from the start of simulation. At that time, the Jeju power system falls to 59.7073 Hz. On the other hand, when 49.5 MW wind farms are connected to each S/S, the Jeju power system falls to 59.6977 Hz. Specifically, the dynamic limit capacity at merit order 1 is determined as 96 MW (48 MW $\times$ 2) because the allowable frequency reference is determined within 59.7 Hz from the Figure 9.

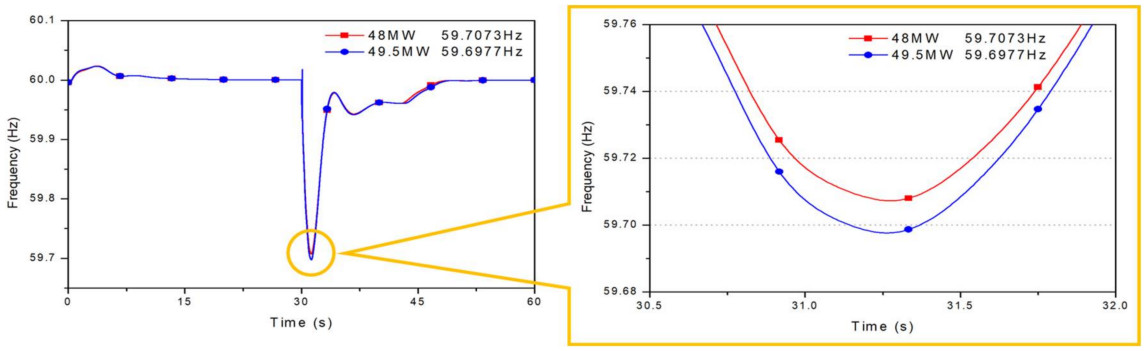

Figure 9. Frequency of Jeju power system on the merit order 1 when the wind farm is lost.

The dynamic limit capacity $P^{D}_{\max}$ of wind farms is determined at the other merit order in the same way as shown in the Figures 10–13. Therefore, the dynamic limit capacity $P^{D}_{\max}$ at each step is determined as follows and is compared between each BESS output control using ROCOF and FDC in the Table 3:

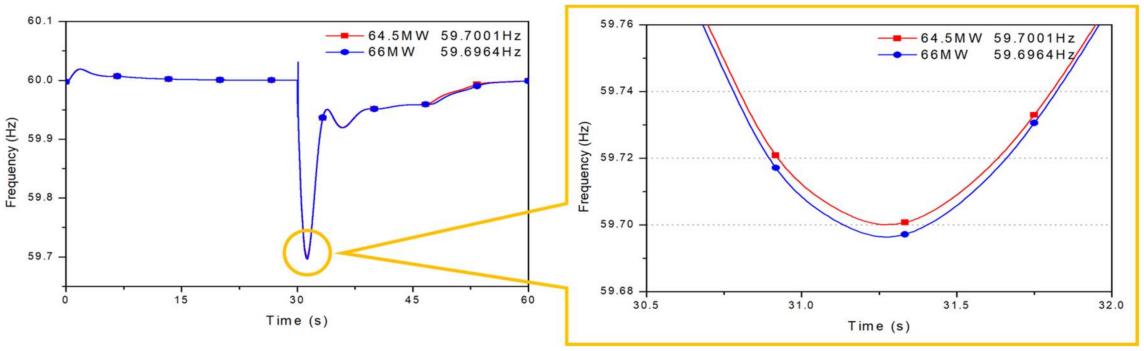

Figure 10. Frequency of Jeju power system on the merit order 2 when the wind farm is lost.

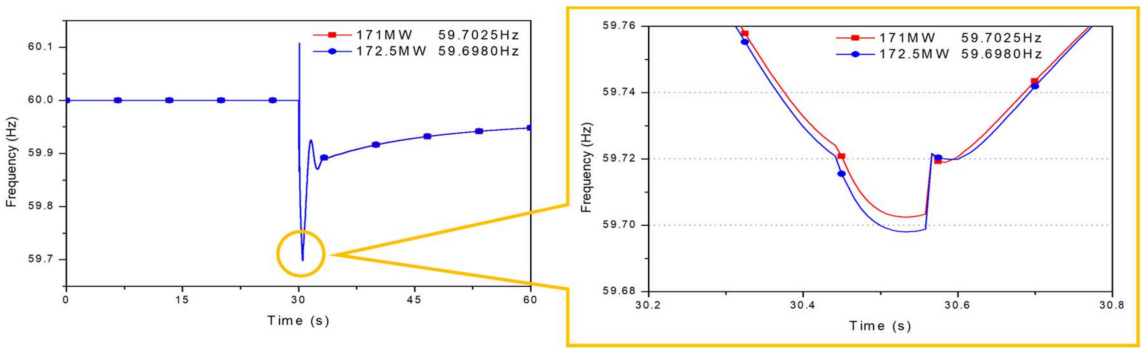

Figure 11. Frequency of Jeju power system at the merit order 3 when the wind farm is lost.

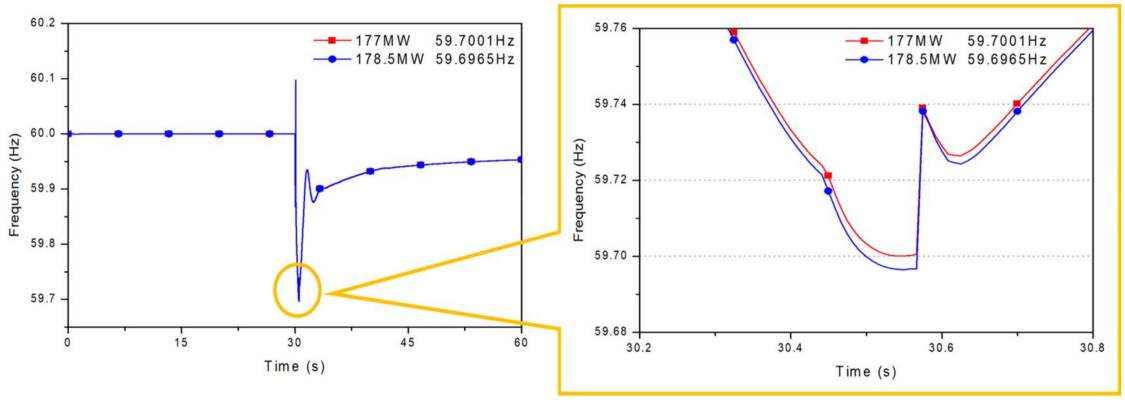

Figure 12. Frequency of Jeju power system at the merit order 4 when the wind farm is lost.

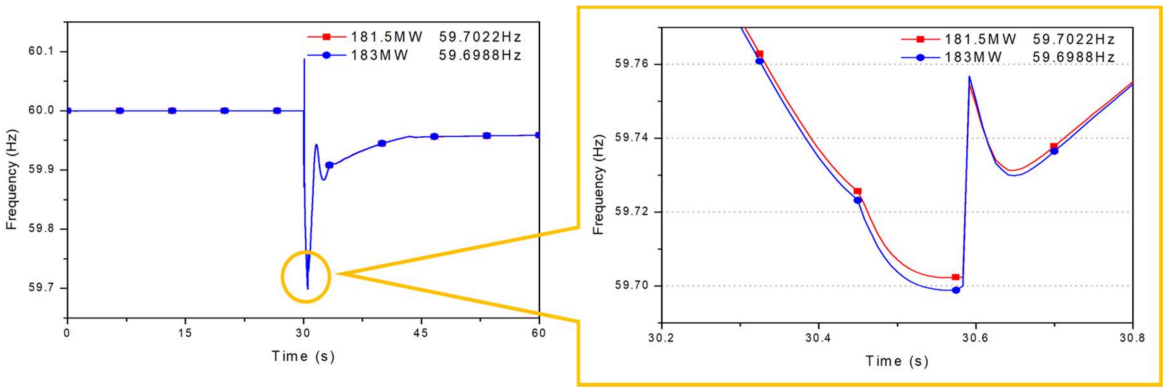

Figure 13. Frequency of Jeju power system at merit order 5 when the wind farm is lost.

Table 3. Dynamic limit capacity of ROCOF and FDC for each merit order.

Dynamic Limit Capacity	ROCOF	FDC
$P^D_{\max}(1)$	96 MW (48 × 2 MW)	84 MW (42 × 2 MW)
$P^D_{\max}(2)$	129 MW (64.5 × 2 MW)	111 MW (55.5 × 2 MW)
$P^D_{\max}(3)$	342 MW (171 × 2 MW)	306 MW (153 × 2 MW)
$P^D_{\max}(4)$	354 MW (177 × 2 MW)	321 MW (160.5 × 2 MW)
$P^D_{\max}(5)$	363 MW (181.5 × 2 MW)	333 MW (166.5 × 2 MW)

Figure 14 shows the dynamic limits of the Jeju island power system with BESS based on ROCOF and FDC, and the system without BESS, with each dynamic limit capacity is determined through the same simulation case. Finally, the operating limit capacity $P^O_{\max}$ of wind farms is set to a lower value between the technical limit capacity $P^T_{\max}$ and the dynamic limit capacity $P^D_{\max}$ for BESS using ROCOF on the system load.

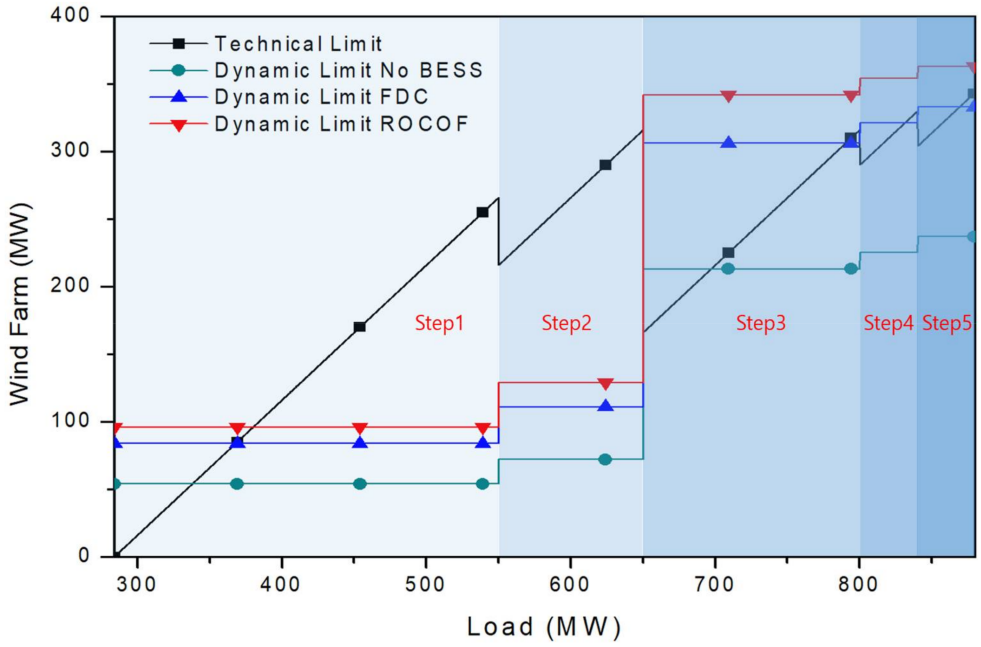

Figure 14. The dynamic limit capacity of wind farms with the technical limit capacity in Jeju island.

3.2. Dynamic Model of Wind Farm

In this paper, PSS/E was used to develop a dynamic model of wind turbine. PSS/E includes a wind turbine package, which provides libraries for various wind turbine manufactures, including Acciona, Enercon, Fuhrlaender, GE, Mitsubishi, Siemens and Vestas. Since doubly fed induction generators (DFIGs) are one of typical wind generator models installed in the Jeju power system, the wind farm in this paper was composed of GE 1.5 MW DFIGs, and hence detailed data and documentation on the DFIGs were available [27,36]. With PSS/E, the multiple wind turbines in a wind farm are modeled as a single representative wind turbine with a common pitch angle. Therefore, for Jeju power system (shown in Figure 1), we used a single 112.5 MW to describe the 75 EA, 1.5 MW wind turbines in the wind farm, which was connected to the Hanrim and Seongsan S/S.

The wind speed was initially maintained constant at 10.5 m/s. At 90 s, the wind speed was decreased to 6.5 m/s over a period of 5 s. This resulted in a decrease in the output power of the Hanrim wind farm from 98 MW to 25 MW. We also considered an increase in the wind speed. The wind speed was initially kept constant at 10.5 m/s and later increased to 14.5 m/s over a period of 5 s. This resulted in an increase in the output power of the Hanrim wind farm from 98 MW to 112.5 MW. We also considered wind speeds from 10.5 m/s to 8.5 m/s, 9.5 m/s, 11.5 m/s and 12.5 m/s, and the Figure 15 shows the result. As expected, the output power of Hanrim wind farm decreased with decreasing wind speed and increased with increasing wind speed.

The output power of Hanrim wind farm did not reach its rated power despite sufficient wind speed. The rated wind speed of the GE 1.5 MW DFIG is 11.5 m/s. and at this speed the output power of Hanrim wind farm should be equal to the rated power of 112.5 MW. However, the output power was only 107.2 MW with a wind speed of 11.5 m/s, as shown in Figure 14b. The pitch angle was 3.66°, which should be decreased to generate more output power. This is because the PSS/E library provides a simplified pitch angle control model for the GE 1.5 MW DFIG. To improve the accuracy of the simulations with variable wind speed, the simplified model of pitch angle control should be modified.

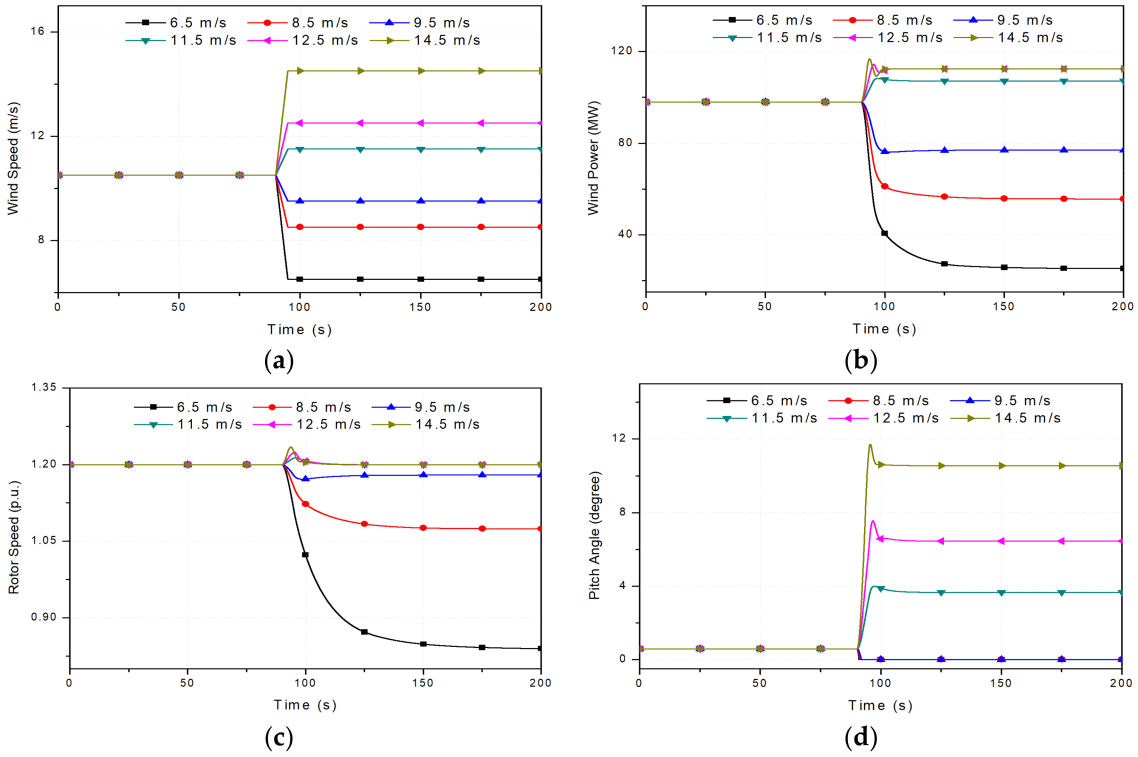

Figure 15. Simulation result with various wind speeds: (**a**) Wind speed; (**b**) Output power; (**c**) Rotor speed; (**d**) Pitch angle.

The wind farms in the Jeju power system will operate based on the operating limit capacity $P^{O}_{\max}$ as presented in Figure 14; therefore, the output power should be controlled, which can be implemented using pitch angle control. As shown in Figure 16, the pitch angle control model for the GE 1.5 MW DFIGs has two controllable parameters: speed and power references [27]. Because PSS/E does not provide a control model for the speed and power references, user-defined models were developed using the model-writing functionality of PSS/E.

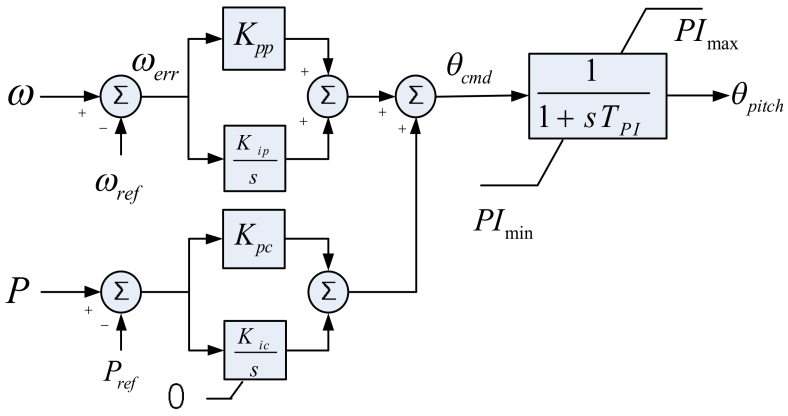

Figure 16. Pitch angle control model of the GE 1.5 MW DFIG.

3.2.1. Pitch Angle Control Based on Speed Reference

Rotor speed control of a DFIG wind turbine is fairly complex [36]. For modeling purposes, this was approximated by closed loop control, with a speed reference that is proportional to the output power, as shown in Figure 17.

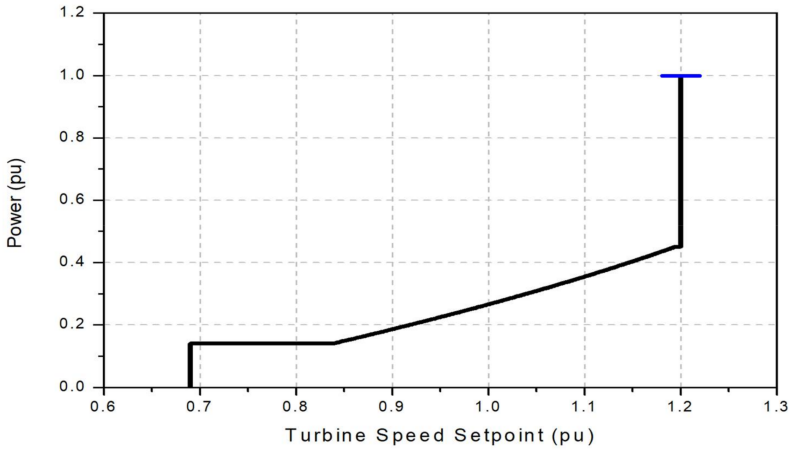

Figure 17. Relationship between the rotor speed set point and the output power of the GE 1.5 MW DFIG model.

The speed reference is normally 1.2 pu; however, this was reduced to the output power below 0.46 pu This behavior was described using the library model with the following relationship, so that the speed reference is given by:

$$\omega_{ref} = -0.75P^2 + 1.59P + 0.63, \qquad P \leq 0.46 \tag{21}$$

The speed reference slowly tracks the changes in output power using a low-pass filter with a time constant of 5 s. The model includes a trip for low rotor speeds: if the rotor speed falls below 0.69 pu, the wind turbine cuts out instantaneously. The model includes cut-in and cut-out threshold wind speeds of 3 m/s and 25 m/s, respectively.

For the output power above the rated (1.0 pu) value, the rotor speed should be controlled such that the output power be equal to the rated power, with the speed being allowed to rise above the reference transiently. This behavior was implemented using the user defined model for the speed reference control as follows:

$$\omega_{ref} = \begin{cases} 0.00 & 0.00 \leq P \leq 0.14 \\ -0.75P^2 + 1.59P + 0.63 & 0.14 < P \leq 0.46 \\ 1.20 & 0.46 < P \leq 1.00 \\ 1.20 + (1.0 - P) \cdot \theta_{pitch} & 1.00 < P \end{cases} \tag{22}$$

where θ_{pitch} is the pitch angle of the wind turbine. Figure 18 shows the simulation results with speed reference control. As expected, it was found that the output power of the Hanrim wind farm was equal to the rated power of 112.5 MW when the wind speed was 11.5 m/s or more.

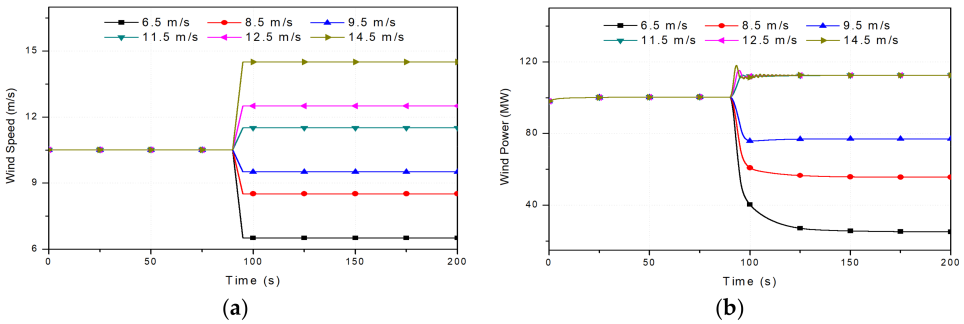

(**a**) (**b**)

Figure 18. *Cont.*

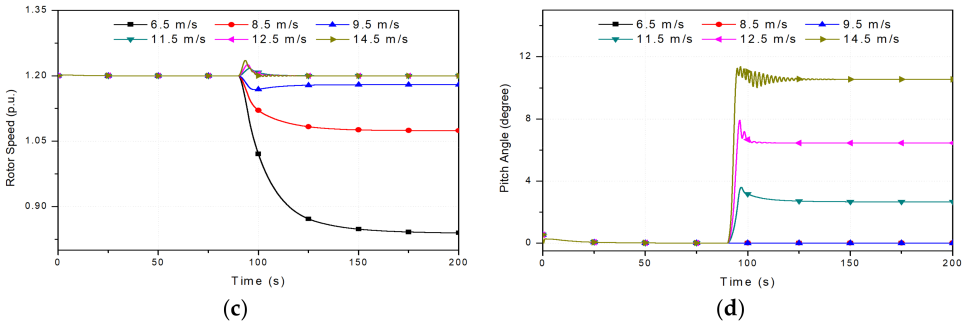

Figure 18. Simulation results with speed reference control: (**a**) Wind speed; (**b**) Output power; (**c**) Rotor speed; (**d**) Pitch angle.

3.2.2. Pitch Angle Control Based on Power Reference

The wind turbine controller regulates the output power of the corresponding wind turbine using the operating limit. This regulation can be implemented using pitch angle control based on the power reference. Figure 16 shows pitch angle control of a wind turbine based on both power and speed reference. The wind turbine controller enables us to use a single representative wind turbine to describe the entire wind farm, so that the power reference of this wind farm was controlled to regulate the output power of the wind farm.

Pitch angle control by power reference determines the power generation rate of the wind turbine. When wind speed is sufficiently high, the wind turbine regulates the pitch angle to limit the output according to the input power reference. Therefore, even if the wind speed is sufficient for the rated power of wind turbine, the output should be limited by the power reference through the pitch angle control.

Figure 19 shows that the wind farm output with the rated power of 48 MW is limited by the power reference. At 50 s, the wind speed is increased to allow the wind turbine to output its rated power. The wind turbine can output the rated power when the wind speed is 11.5 m/s or more [27]. However, the wind farm output is limited to 43.2 MW by pitch angle control because the power reference is 0.9 pu. Thus, the output of the wind turbine can be controlled according to the operating limit.

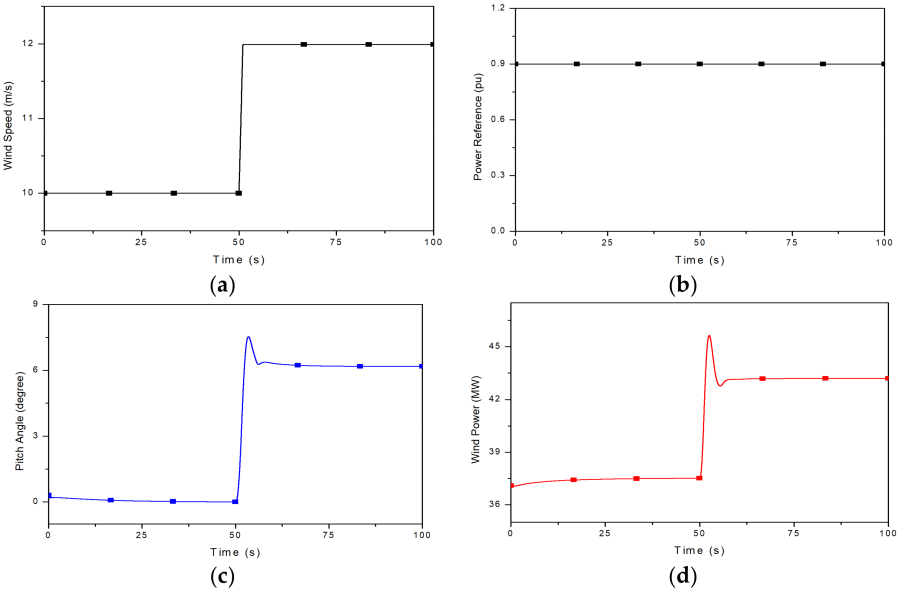

Figure 19. Simulation results with power reference: (**a**) Wind speed; (**b**) Power reference; (**c**) Pitch angle; (**d**) Wind power.

4. Case Study: Wind Farms with BESS in Jeju Island

The BESS output control method proposed in the previous section was used to determine the operating limit capacity of the wind farms, and it was confirmed that the wind farm output was controlled according to the power reference. In this section, we will confirm the wind farm output and BESS for changes of wind speed and load. The wind turbine should be able to control the output according to the operating limit capacity, and BESS should be able to compensate quickly for the insufficient power between supply and demand caused by the disturbance.

4.1. Output Control of Wind Farm and BESS on Wind Speed Increase

For the simulation, Jeju island power system is used, that is constructed as shown in the Figure 1. In Figure 14, the operating limit capacity of wind farms at merit order 1 is 96 MW, with 48 MW installed at each of Seongsan S/S and Hanrim S/S. The rated power of the other synchronous generators in merit order 1 is 550 MW (refer to Table 2); therefore, the rated power of BESS can be calculated as in Section 2.1:

$$P_{BESS} = 0.495P_W - 0.005P_{SG} = 0.495 \times 48 - 0.005 \times 550 \cong 21 \text{ MW} \quad (23)$$

BESS is connected to Hanrim S/S, the initial pure load was set as 356 MW and the initial wind speed as 10 m/s, and the wind farm output was 37.5 MW and an initial BESS output of 0 MW. At a load of 356 MW, the power reference of wind turbine should be 0.75 pu, but this value that does not consider the loss in the power system. The total system load is the sum of the system load and loss; however, since it is practically difficult to measure the system load and loss, the system total load is determined by the amount of power of penetrated generators.

Figure 20 shows the simulation results with power reference control in addition to speed reference control. When the total load was 369.6 MW (i.e., a pure load of 356.5 MW and losses of 13.1 MW), the technical limit capacity of the Jeju power system was 85.6 MW, which was calculated using (15). As there were two wind farms with the same rated power of 48 MW, the operating limit capacity of Hanrim wind farm was 42.8 MW and the power reference was set to 0.8917 pu (i.e., 42.8 MW/48.0 MW). The wind speed was initially maintained constant at 10 m/s, and at 50 s was increased to 12.0 m/s over a period of 1 s. The output power of a wind farm should not exceed the operating limit capacity, even though the wind speed was sufficient to generate more output power. Therefore, the output power of Hanrim wind farm was limited to 42.8 MW due to the operating limit capacity, as shown in Figure 20d.

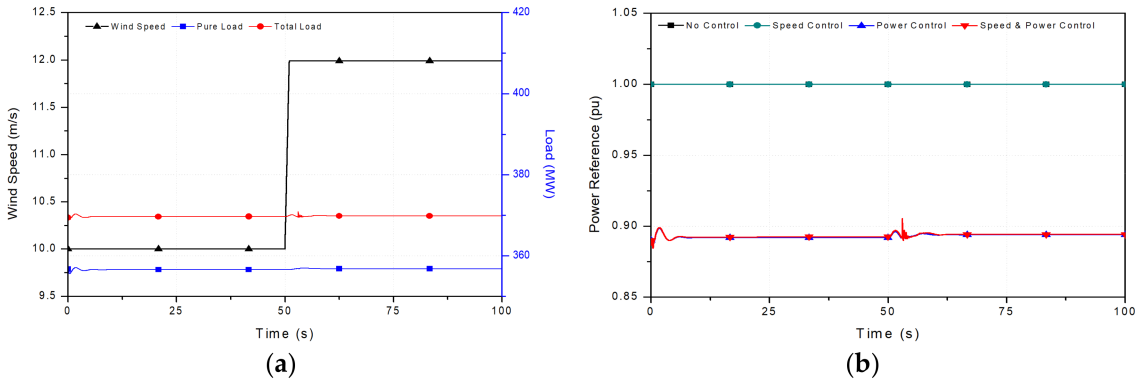

Figure 20. *Cont.*

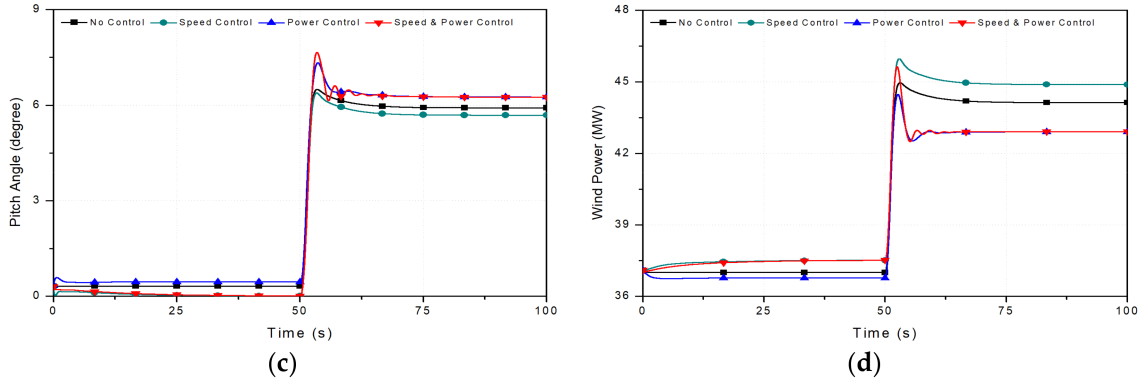

Figure 20. Simulation result when wind speed is increased (0~100 s): (**a**) Wind speed and loads; (**b**) Power reference; (**c**) Pitch angle; (**d**) Output of wind turbine.

Figure 21 shows frequency and BESS output with FDC and ROCOF respectively. The instantaneous frequency fluctuation occurs for wind speed increase, and BESS is also charged and discharged accordingly. However, BESS output control using ROCOF does not demonstrate any advantage over FDC for the frequency regulation when the frequency fluctuation is small.

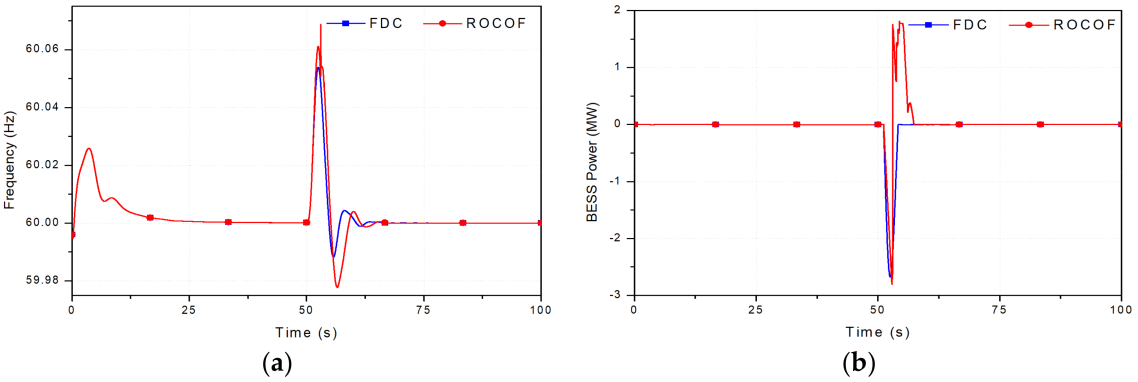

Figure 21. BESS output and frequency result when wind speed is increased (0~100 s): (**a**) Frequency; (**b**) BESS output.

4.2. Output Control of Wind Turbine and BESS on Load Increase

Figure 22 shows the simulation results when the total load of the Jeju power system increased. Here, the wind speed was maintained constant at 12.0 m/s after 51 s, and a total load of Jeju power system increased from 369.6 MW to 377.9 MW at 100 s. This increase in the total load resulted in an increase in the operating limit capacity of the Hanrim wind farm from 42.80 MW to 46.95 MW. Consequently, the power reference of the Hanrim wind farm increased from 0.8917 pu to 0.9780 pu (i.e., 46.95 MW/48.0 MW). As expected, the output power of the Hanrim wind farm was successfully limited to 46.95 MW. At 150 s, there was an additional increase in the total load from 377.9 MW to 397.5 MW. This caused the operating limit capacity of the Hanrim wind farm to follow the dynamic limit capacity of 48.0 MW. Meanwhile, the power reference of the Hanrim wind farm increased from 0.9780 pu to 1.0 pu. As expected, the output power of the Hanrim wind farm increased to the rated power, 48 MW.

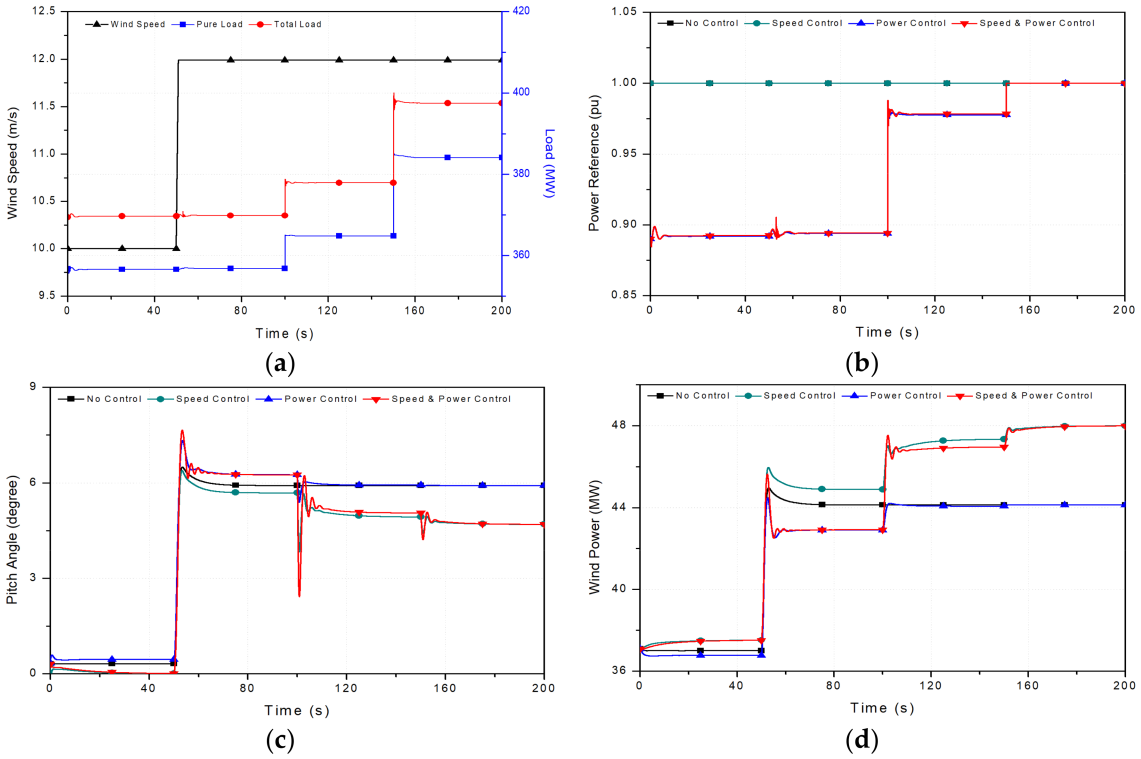

Figure 22. Simulation results when the power system load is increased (0~200 s): (**a**) Wind Speed and loads; (**b**) Power reference; (**c**) Pitch angle; (**d**) Output of wind turbine.

Figure 23 also shows frequency and BESS output with FDC and ROCOF when the power system load is increased. The increased loads are satisfied with the ROCOF threshold, and BESS using ROCOF more quickly compensates for insufficient power than FDC. Fast power compensation can reduce the instantaneous frequency deviation.

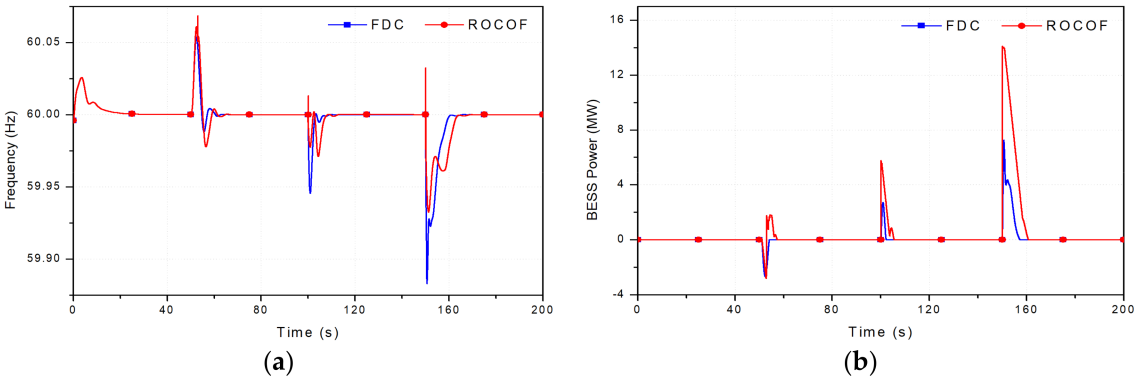

Figure 23. BESS effects when the load is increased (0~200 s): (**a**) Frequency; (**b**) BESS output.

5. Conclusions

This paper has determined the rated power of BESS and the operating limit capacity of wind farms for the power system. A novel control scheme is described for a BESS using ROCOF and wind farms based on the operating limit capacity in the power system. To determine the rated power of BESS, the maximum deviation of kinetic energy is used in the operation range of the power system frequency. The rated power of BESS is determined by compensating the maximum deviation of kinetic energy as BESS in the operation range of the power system frequency. Furthermore, to improve the

system stability, the power deviation between supply and demand is more quickly compensated by the proposed BESS output control method. In Section 2, the simulation results have showed that the BESS using ROCOF control can raise the frequency nadir by compensating for the power deviation more quickly than FDC after transient.

The operating limit capacity was defined as the minimum of the technical and dynamic limit capacity. The technical limit capacity was determined mainly by the characteristics of the generating units including two pairs of HVDC lines. The dynamic limit capacity was considered using the simulation of the case of sudden loss of wind power generation. The calculated operating limit capacity is the reference for the output of wind turbines, which is controlled by the pitch angle. To confirm the result, PSS/E was used to develop the dynamic model of a wind turbine composed of GE 1.5 MW DFIGs. The pitch angle control of wind turbine consists of the two controllable parameters, which were the speed and power references. As PSS/E does not provide a control model for the speed and power references, user-defined models were developed for the speed and power references. Speed reference control was used to provide accurate simulations in which the wind speed was varied and power reference control was used to implement the operating limit capacity. In the Section 4, the simulation results have shown that the appropriate power of wind farm was output by pitch angle control to response to variations in the wind speed and the total load of the power system.

As the research progresses, we could have increased the operating limit capacity of wind farms by calculating the appropriate rated power of BESS and controlling the output of BESS using ROCOF, and confirmed the usefulness of the operation of proposed BESS and wind farm by controlling the output of wind turbine according to the operating limit capacity.

Acknowledgments: This research was supported in part by the Human Resources Program in Energy Technology of the Korea Institute of Energy Technology Evaluation and Planning (KETEP), and granted financial resources from the Ministry of Trade, Industry & Energy, Republic of Korea (No. 20154030200770). This research was also supported in part by Korea Electric Power Corporation. (Grant number: R17XA05-2)

Author Contributions: Dae-Hee Son prepared the manuscript and completed the methodology and the simulations. Soon-Ryul Nam supervised the study and coordinated the main theme of this paper. Muhammad Ali, Sang-Hee Kang and Jae-Haeng Heo discussed the results and implications, and commented on the manuscript. All of the authors read and approved the final manuscript.

Conflicts of Interest: The authors declare no conflict of interest.

References

1. Global Wind Energy Council (GWEC). *Global Wind Report 2016*; GWEC: Ulaanbaatar, Mongolia, 2017; p. 13.
2. Korea Power Exchange (KPX). The 8th Basic Plan for Long-Term Electricity Supply and Demand (2017–2031). Available online: https://www.kpx.or.kr/eng/index.do (accessed on 29 December 2017).
3. Kim, E.H.; Kim, J.H.; Kim, S.H.; Choi, J.H.; Lee, K.Y.; Kim, H.C. Impact Analysis of Wind Farms in the Jeju Island Power System. *IEEE Syst. J.* **2015**, *6*, 134–139. [CrossRef]
4. Lee, K.Y.; Kim, S.H. Progress in distributed generation in Korea. In Proceedings of the 2007 IEEE Power Engineering Society General Meeting, Tampa, FL, USA, 24–28 June 2007; pp. 1–6.
5. 100% Renewable Energy Is a Reality Today. Jeju Province, Korea. Available online: www.go100re.net/properties/jeju-province-korea/ (accessed on 3 August 2016).
6. Chen, Z. Issues of Connecting Wind Farms into Power Systems. In *Transmission and Distribution Conference and Exhibition*; Asia and Pacific: Dalian, China, 18 August 2005.
7. Palsson, M.P.; Toftevaag, T.; Uhlen, K.; Tande, J.O.G. Large-scale Wind Power Integration and Voltage Stability Limit in Regional Networks. In Proceedings of the Power Engineering Society Summer Meeting, Chicago, IL, USA, 21–25 July 2002.
8. EL-Shimy, M.; Badr, M.A.L.; Rassem, O.M. Impact of Large Scale Wind Power on Power System Stability. In Proceedings of the 12th International Middle-East Power System Conference, MEPCON 2008, Aswan, Egypt, 12–15 March 2008.
9. Papathanassiou, S.A.; Boulaxis, N.G. Power limitations and energy yield evaluation for wind farms operating in island systems. *Renew. Energy* **2006**, *31*, 457–479. [CrossRef]

10. Park, J.W.; Park, Y.H.; Moon, S.I. Instantaneous Wind Power Penetration in Jeju Island. In Proceedings of the Power and Energy Society General Meeting—Conversion and Delivery of Electrical Energy in the 21st Century, Pittsburgh, PA, USA, 20–24 July 2008.
11. *Energy Storage World Markets Report 2014–2020*. Download from Energy Storage World Forum. Available online: http://energystorageforum.com/ (accessed on 8 May 2017).
12. Kottick, D.; Blau, M.; Edelstein, D. Battery energy storage for frequency regulation in an island power system. *IEEE Trans. Energy Convers.* **1993**, *8*, 455–459. [CrossRef]
13. Oudalov, A.; Chartouni, D.; Ohler, C. Optimizing a Battery Energy Storage System for Primary Frequency Control. *IEEE Trans. Power Syst.* **2007**, *22*, 1259–1266. [CrossRef]
14. Delille, G.; François, B.; Malarange, G. Dynamic frequency control support: A virtual inertia provided by distributed energy storage to isolated power systems. In Proceedings of the Innovative Smart Grid Technologies Conference Europe, Gothenberg, Sweden, 11–13 October 2010.
15. Han, Y.; Young, P.M.; Jain, A.; Zimmerle, D. Robust Control for Microgrid Frequency Deviation Reduction with Attached Storage System. *IEEE Trans. Smart Grid* **2015**, *6*, 557–565. [CrossRef]
16. Liu, J.; Wen, J.; Yao, W.; Long, Y. Solution to short-term frequency response of wind farms by using energy storage systems. *IET Renew. Power Gener.* **2016**, *10*, 669–678. [CrossRef]
17. Serban, I.; Marinescu, C. Battery energy storage system for frequency support in microgrids and with enhanced control features for uninterruptible supply of local loads. *Int. J. Electr. Power Energy Syst.* **2014**, *54*, 432–441. [CrossRef]
18. Huang, X.; Jin, X.; Ma, T.; Tong, Y. A voltage and frequency droop control method for microsources. In Proceedings of the International Conference on Electrical Machines and Systems (ICEMS), Beijing, China, 20–23 August 2011.
19. Ayman, B.A.; José, L.D.G.; Bianchi, F.D.; Olimpo, A.L. Enhancing frequency stability by integrating non-conventional power source through multi-terminal HVDC grid. *Int. J. Electr. Power Energy Syst.* **2018**, *65*, 128–136. [CrossRef]
20. Shuthakini, P.; Joseph, E.T. Energy Storage System Control for Prevention of Transient Under-Frequency Load Shedding. *IEEE Trans. Smart Grid* **2017**, *8*, 927–936. [CrossRef]
21. Knap, V.; Sinha, R.; Swierczynski, M.; Stroe, D.; Chaudhary, S. Grid inertial response with Lithium-ion battery energy storage systems. In Proceedings of the IEEE 23rd International Symposium on Industrial Electronics (ISIE), Istanbul, Turkey, 1–4 June 2014.
22. Adrees, A.; Milanovic, J.V. Study of frequency response in power system with renewable generation and energy storage. In Proceedings of the Power System Computation Conference (PSCC), Genoa, Italy, 20–24 June 2016.
23. Zhang, J.; Cheng, M.; Chen, Z.; Fu, X. Pitch angle control for variable speed wind turbines. In Proceedings of the Third International Conference on Electric Utility Deregulation and Restructuring and Power Technologies (DRPT), Nanjing, China, 6–9 April 2008.
24. Muljadi, E.; Butterfield, C.P. Pitch-controlled variable-speed wind turbine generation. *IEEE Trans. Ind. Appl.* **2001**, *37*, 240–246. [CrossRef]
25. Slootweg, J.G.; Polinder, H.; Kling, W.L. Dynamic modelling of a wind turbine with doubly fed induction generator. In Proceedings of the Power Engineering Society Summer Meeting, Vancouver, BC, Canada, 15–19 July 2001.
26. Yilmaz, A.S.; Özer, Z. Pitch angle control in wind turbines above the rated wind speed by multi-layer perceptron and radial basis function neural networks. *Expert Syst. Appl.* **2009**, *36*, 9767–9775. [CrossRef]
27. Kazachkov, Y.; Keung, P.K.; Patil, K. *PSS/E Wind Modeling Package for GE 1.5/3.6/2.5 MW Wind Turbines, Issue 5.1.0*; Siemens Power Technologies International: New York, NY, USA, 2009.
28. Siemens Energy, Inc. Power Technologies International. Chapter 1—Generator Model Data Sheets. In *PSS/E 32.0.5 PSS/E MODEL LIBRARY*; Siemens Energy, Inc.: New York, NY, USA, October 2010; pp. 11–58.
29. Siemens Energy, Inc. Power Technologies International. Chapter 20—Model Writing. In *PSS/E 32.0.5 Program Operation Manual*; Siemens Energy, Inc.: New York, NY, USA, October 2010; pp. 1353–1378.
30. Siemens Energy, Inc. Power Technologies International. Chapter 12—Dynamic Simulation Principles. In *Program Application Guide*; Siemens Energy, Inc.: New York, NY, USA, October 2010; Volume 2, pp. 29–56.
31. Son, D.H.; Kang, S.H.; Nam, S.R. Dynamic Modeling of Wind Farms in the Jeju Power System. *Int. J. Electr. Comput. Energ. Electron. Commun. Eng.* **2016**, *10*, 508–512.

32. North American Electric Reliability Corporation (NERC). BAL-003-1—Frequency Response and Frequency Bias Setting. Reliability Standards for the Bulk Electric Systems of North America. Available online: https://www.nerc.com/ (accessed on 5 November 2014).
33. Erinmez, I.A.; Bickers, D.O.; Wood, G.F.; Hung, W.W. NGC experience with frequency control in England and Wales-provision of frequency response by generators. In Proceedings of the IEEE Power Engineering Society Winter Meeting, New York, NY, USA, 31 January–4 February 1999.
34. North American Electric Reliability Corporation (NERC). BAL-001-1—Primary Frequency Response in the ERCOT Region. Reliability Standards for the Bulk Electric Systems of North America. Available online: https://www.nerc.com/ (accessed on 5 November 2014).
35. Siemens Energy, Inc. Power Technologies International, Chapter 24—Other Models. In *Program Application Guide*; Siemens Energy, Inc.: New York, NY, USA, October 2010; Volume 2, pp. 551–596.
36. Clark, K.; Miller, N.W.; Sanchez-Gasca, J.J. *Modeling of GE Wind Turbine-Generators for Grid Studies, Version 4.3*; General Electric International, Inc.: New York, NY, USA, 2009; pp. 31–35.